

The therapeutic effects of Hexuetongbi formula to combat the oxaliplatin-induced peripheral neuropathy using network pharmacological methods in rat model

Jingyu Feng^{1,2}, Li Yang¹, Jiguo Wang^{1,2}, Jing Zhang^{1,2}, Lizhu Lin^{2,3*}

¹Department of Oncology, Shenzhen Bao'an Traditional Chinese Medicine Hospital, Shenzhen 518133, China

²The First School of Clinical Medicine, Guangzhou University of Traditional Chinese Medicine, Guangzhou 510405, Guangdong, China

³Department of Oncology, The First Affiliated Hospital of Guangzhou University of Traditional Chinese Medicine, Guangzhou 510405, Guangdong, China

Received:

November 22, 2023

Accepted:

May 28, 2024

Published Online:

July 12, 2024

Abstract

The objective of this study was to elucidate the mechanism of the Hexuetongbi formula in treating Chemotherapy-induced Peripheral Neuropathy (CIPN) using network pharmacology, pharmacodynamics, and mechanistic approaches in an oxaliplatin-induced peripheral neuropathy rat model. Network pharmacology is crucial for understanding the multi-target effects of the Hexuetongbi formula on CIPN. This approach allows for a comprehensive mapping of the complex interactions between the formula's constituents and the biological pathways involved in CIPN, revealing potential synergistic effects and enhancing the formula's pharmacological validation. The Hexue Tongbi formula's impact was analyzed on rats undergoing peripheral neuropathy, observing changes in the morphology of L4-6 dorsal root ganglion neurons through hematoxylin and eosin (HE) staining. Simultaneously, a network pharmacology approach was employed, utilizing TCMSP and GeneCards databases to identify common targets between CIPN and Hexue Tongbi's therapeutic entities. These core targets were scrutinized through GO enrichment and KEGG pathway analysis. To validate the findings, mRNA and protein expression levels in the L4-6 dorsal root ganglion were examined using quantitative PCR and Western Blot assays. Significant modifications were observed in the frequency of cold stimulus withdrawal reflexes and the L4-6 dorsal root ganglion neurons, while the mechanical withdrawal reflex threshold displayed a considerable decrease. In rats treated with the Hexuetongbi formula post-oxaliplatin, there was noteworthy mitigation in the cold stimulation paw withdrawal threshold and augmentation in the mechanical stimulation paw withdrawal threshold. Network pharmacology identified 19 active constituents in Hexuetongbi and 35 targets for CIPN, with the PI3K/Akt signaling pathway emerging as a prominent target. There was a significant upregulation in PI3K, Akt1, Akt2, and Bcl-2 compared to controls, suggesting that Hexuetongbi effectively mitigates oxaliplatin-induced peripheral neuropathy through the modulation of the PI3K/Akt and Bcl-2 pathways.

Keywords: Oxaliplatin, Chemotherapy-induced peripheral neuropathy, Traditional Chinese medicine, Dorsal root ganglion, Apoptosis

How to cite this:

Feng J, Yang L, Wang J, Zhang J and Lin L. The therapeutic effects of Hexuetongbi formula to combat the oxaliplatin-induced peripheral neuropathy using network pharmacological methods in rat model. Asian J. Agric. Biol. 2024(4): 2023321. DOI: <https://doi.org/10.35495/ajab.2023.321>

*Corresponding author email:
15706345@163.com

This is an Open Access article distributed under the terms of the Creative Commons Attribution 4.0 License. (<https://creativecommons.org/licenses/by/4.0>), which permits unrestricted use, distribution, and reproduction in any medium, provided the original work is properly cited.



Introduction

Chemotherapy-Induced Peripheral Neuropathy (CIPN) is the most prevalent non-hematological adverse effect observed in patients undergoing chemotherapy, especially those administered anti-cancer drugs containing platinum compounds, tubulin inhibitors, and glutamic acid derivatives (Argyriou et al., 2012). Research indicates that oxaliplatin, a chemotherapeutic agent, has the highest incidence of causing CIPN, with a 92 percent incidence rate across all grades of chemotherapy-induced peripheral neuropathy (Delaunoy et al., 2005). Oxaliplatin damages the dorsal root ganglion, leading to acute and chronic neurotoxicity (Argyriou et al., 2012).

It is hypothesized that the acute neurotoxicity of oxaliplatin stems from abnormal sodium ion channel activity on the axonal cell surface, impacting the voltage-dependent sodium ion channels and prolonging the opening of Na⁺ channels, which results in nerve overexcitation, potentially leading to paresthesia and muscle tremors (Argyriou, 2015). In contrast, the precise mechanism behind oxaliplatin's chronic neurotoxicity remains elusive, but it is suspected to relate to its accumulation in the dorsal root ganglia, causing apoptosis (Argyriou et al., 2008; Mannelli et al., 2012).

Oxaliplatin, a platinum-based chemotherapy agent, is widely utilized as an effective treatment for pancreatic, colorectal, and gastric cancers and is commonly used in combination with therapeutic agents like irinotecan, fluorouracil, tegafur, capecitabine, oteracil and gimeracil (Heinemann et al., 2012; Liu et al., 2022; Nara et al., 2023; Sasako et al., 2011). Nevertheless, it frequently induces severe peripheral neuropathy, impacting the patient's quality of life and, in extreme cases, necessitating treatment discontinuation, subsequently affecting patient survival.

Several treatment options, such as cytoprotective agents, glutamine, a calcium-magnesium mixture, and vitamin E, have been explored to alleviate CIPN (Staff et al., 2017). Unfortunately, recent studies have demonstrated that the calcium-magnesium combination significantly fails to alleviate or prevent oxaliplatin-induced peripheral neuropathy (Gamelin et al., 2008; Hochster, 2007; Loprinzi et al., 2014). A meta-analysis showed no clinical evidence supporting the efficacy of several potentially protective drugs, including amifostine and glycylamide (Albers et al., 2014).

Duloxetine has been recommended for CIPN treatment in the 2014 ASCO guidelines but is associated with side effects (Hershman et al., 2014). The limited understanding of the mechanism of nerve damage induced by oxaliplatin and the absence of a suitable genetic target impede the development of effective treatments for CIPN.

The ASCO guidelines suggest that traditional Chinese medicine (Kampo medicine) could serve as a potential therapeutic alternative for preventing and treating CIPN, although substantial published data supporting this are lacking. The Hexuetongbi formula, a traditional Chinese medicine recipe consisting of five herbs: Chuanwu, Asarum, Chuanmutong, Guizhi, and Angelica, has been observed to affect the treatment of CIPN through external washing significantly; however, its pharmacological mechanism remains unidentified.

CIPN is a debilitating side effect of many oncological treatments, affecting a significant proportion of cancer survivors. The onset of CIPN can severely impact a patient's quality of life and may necessitate dose reductions or discontinuation of chemotherapy, compromising cancer treatment efficacy. Current interventions, such as the use of the antidepressant duloxetine, have shown some efficacy in managing this condition but are often limited by side effects and variable patient responses (Smith et al., 2013).

Despite these options, many patients continue to experience substantial pain and discomfort, leading researchers to explore additional therapeutic strategies, including Traditional Chinese Medicine (TCM). TCM and integrative approaches, such as acupuncture, have been increasingly recognized for their potential to alleviate symptoms of CIPN. Recent systematic reviews and randomized controlled trials have provided preliminary evidence supporting the effectiveness of these approaches, suggesting that acupuncture could significantly reduce CIPN symptoms in cancer survivors (Chien et al., 2019; Lu et al., 2020).

To unravel this, our investigation employed network pharmacology, pharmacodynamics, and mechanistic approaches to explore the mechanism of Hexuetongbi Formula in addressing CIPN and any underlying molecular mechanisms that might influence the treatment of CIPN. More research is pivotal for identifying precise genetic markers and developing effective drugs to mitigate this side effect.



Material and Methods

The Hexuetongbi formula is composed of five types of traditional Chinese medicine: Chuanwu (10 g), Guizhi (10 g), Asarum (10 g), Chuanmutong (10 g), and Angelica (10 g). The laboratory at Guangzhou University of Chinese Medicine formulated liquid extracts from these five medicinal components, sourced from the Chinese Pharmacy of the First Affiliated Hospital of Guangzhou University of Chinese Medicine (Kangmei Pharmaceutical, batch numbers: 19020117, 190403, 190401, 190701, G5219921), and achieved an extract concentration of 30g/L.

Oxaliplatin (batch number: 190201) was procured from Hainan Jinrui Pharmaceutical Co., Ltd. It was prepared by adding 50 mg of oxaliplatin to 250 mL of a 5% glucose solution to attain a final 0.2 mg/mL concentration. Additionally, products such as 4% paraformaldehyde, hematoxylin, and eosin staining kit, paraffin, neutral gum mounting media, and xylene (Product numbers: E672002-0500, A530011-0500, A606115-0250, E607318 -0200, E675007-0100) were acquired from Shanghai Sangon Bioengineering Co., Ltd.

Table-2: Primer sequences

Primer Name	Forward Sequence	Reverse Sequence
PI3K	CTGGAGAGCTTGGAGGACGA	TCGCAAGAACCAGAATAAGAAGTG
Akt1	AATACCTGGTGTCGGTCTCA	TCGAGCTCATCCTAATGGAG
Akt2	GGCCCCGGTACTTCCTTC	TAGCCCGTATCCACTCTCCCTCTC
Akt3	TGGCACCAGAGGTATTAGAAG	TATCAAGAGCCCTGAAAGCAA
MAPK8	CCACCACCAAAGATCCCTGACAAG	TCATCTACAGCAGCCAGAGGTC
PTGS2	TGTATCCCGCCCTGCTGGTG	CGTTGATGGTGGCTGTCTTGGTAG
Bcl-2	ACGGTGGTGGAGGAACCTTCAG	TTCAGAGACAGCCAGGAGAAATCAAAC

A Real-Time PCR Kit (Cat. No.: RR820A) was purchased from TAKARA, Japan, and Real-time RT-PCR primers (refer to Table 2) were designed and synthesized by Sangon Bioengineering (Shanghai) Co., Ltd. The BCA Protein Content Detection Kit (Cat. No.: P0010) was sourced from Beyotime Biotechnology, Shanghai, China. Various antibodies including anti-GAPDH Rabbit

mAb (Cat. No.: AF0911, Affinity Biosciences LTD), Goat Anti-Mouse IgG (Cat. No.: BA1050, Boster Biological Technology Co. Ltd), Goat Anti-Rabbit IgG (Cat. No. BA1054, Boster Biological Technology Co. Ltd), Anti-Bcl-2 Antibody (Cat. No. ab196495, Abcam), Anti-PI3 Kinase p110 beta Antibody [EPR5515(2)] (Abcam), Anti-AKT (Cat. No. ab151549, Abcam), and phosphor-S473 Antibody [EP2109Y] (Cat. No. ab81283, Abcam) were also purchased.

Animals used

We acquired thirty male SD rats of SPF grade, each weighing 200±20g, from Guangzhou Pharmaceutical University. They were originally sourced from the Guangdong Provincial Laboratory Animal Center (license number: SCXK (Guangdong) 2018-0002), with the experimental animal batch number: No.44007200068466.

The rats were accommodated in a serene and hygienic environment equipped with an air filtration system, maintaining a temperature of 20-25°C and 40-60% relative humidity. They had ad libitum access to food and water. The animal laboratory sustained a 12-hour light/dark cycle to simulate a natural environment conducive to the well-being and normal behavior of the animals.

Animal model development and study design

The animal experimentation procedures used in this study received approval from the Animal Ethics Committee and the Experimental Unit at Guangzhou University of Traditional Chinese Medicine under the authorization number SCXK 2017-0125. These procedures adhered to the guidelines established by the National Institutes of Health for the use and care of laboratory animals (National Research Council (US) Committee for the Update of the Guide for the Care and Use of Laboratory Animals, 2011). Thirty SPF SD male rats were segregated into three distinct groups, consisting of ten rats per group: Control group (group C), Model group (group M), and Xuetongbi Recipe bath group (group H).

Group C received intraperitoneal injections of 2 ml of 5% glucose solution. In comparison, rats in groups M and H were administered 2 mL of prepared oxaliplatin solution intraperitoneally twice weekly over four weeks (on the 1st, 2nd, 8th, 9th, 15th, 16th, 22nd, and 23rd days), establishing a standard model for oxaliplatin-induced peripheral neuropathy (Holmes et al., 1998).



For tests involving cold stimuli-induced persistent pain, rats in group H received a Xuotongbi Recipe bath. They were housed in plastic containers with lids, allowing for foot immersion in 2L of a medicinal solution with a concentration of 17g/L and a regulated temperature of 38°C. These animals underwent exposure to -42°C daily for intervals of 30 minutes. The Xuotongbi Recipe bath was administered for 6 consecutive days, followed by a day of rest, totaling a seven-day treatment course, repeated for three courses. Concurrently, animals in groups C and M submerged their feet daily in an equivalent volume of freshwater under identical conditions to group H. Comprehensive examinations were conducted on all groups for general needs and potential toxic reactions throughout the administration period. Weekly assessments included the mechanical stimulation of the foot withdrawal threshold test and the evaluation of persistent pain induced by cold stimulation.

After three weeks, rats were anesthetized with 2% sodium pentobarbital, followed by abdominal dissection and collection of abdominal aortic blood. Subsequently, the dorsal root ganglia of the L4-6 segments were extracted for further experimentation.

Behavioral tests

Toxicity monitoring

Methodologies for detecting toxicity included tests for skin irritation, sensitization, acute toxicity, and chronic toxicity. Variations in the body weight of the rats were meticulously monitored throughout these experiments. Upon conclusion of the investigations, blood samples were collected to analyze the myocardial enzyme spectrum, liver functions, and renal functions.

Mechanical stimulus withdrawal threshold test

This test quantifies mechanical nociception and assesses an animal's capacity to discern a noxious stimulus. In this case, the soles of the rats were subjected to stimulation using an electrical Von Frey pain meter, which records the stimulation intensity in grams. Measurements were taken before the modeling (day 0), before administration, and on days 7, 14, 21, and 28 during administration. During these periods, rats were housed in transparent acrylic cages equipped with metal mesh floors and were allowed to acclimate before undergoing the test.

Each rat's bilateral hind feet were tested five times, maintaining a delay exceeding 6 seconds between

each measurement. Observations were recorded both when the hind feet were stimulated and immediately after the removal of the probe. Immediate foot withdrawals, twitching, foot licking, and other reflexes were considered beyond the purview of the foot withdrawal scope. The probability of positive responses was then calculated, denoted by the number of positive responses out of ten, expressed as a percentage (Zheng et al., 2011).

Cold stimulation-induced persistent pain test

Researchers (Jasmin et al., 1998) conducted detections on the 7th, 14th, 21st, and 28th days prior to modeling and on day 0 before administration. Rats were positioned on a cold plate, maintained at a surface temperature of 41°C, surrounded by a transparent acrylic cage around the plate's perimeter. Before initiating the test, 5 minutes were allocated to allow the rats to acclimate to their new environment. The rats' cumulative count of foot withdrawals, twitching, and foot licking within the 5-minute interval was recorded, excluding the foot lifts induced by the rats' regular activities.

Pathological assessment

After the experiment, dorsal root ganglia from levels L4-6 were extracted, fixed, dehydrated, embedded in paraffin, and sectioned at 5 micrometers along the longitudinal axis. After standard Hematoxylin and Eosin (HE) staining, histomorphological alterations were scrutinized under a microscope. The examined tissue samples exhibited typical pathological modifications, which included inflammation, necrosis, degeneration, hyperplasia, and fibrosis.

Network pharmacology analysis and Xuotongbi recipe

Active ingredients and target genes of each traditional Chinese medicine in the Hexuotongbi recipe

The research employed the Traditional Chinese Medicine Systems Pharmacology Database and Analysis Platform (TCMSP) to identify all the chemical components in the Xuotongbi formula, a combination of five traditional Chinese medicines. The screening criteria included a bioavailability (OB) of $\geq 30\%$ and drug-like properties (DL) of ≥ 0.18 (Liu et al., 2013). Subsequently, compounds aligning with these conditions were aggregated, with TCMSP discerning the pertinent target genes from the derived active components.



Disease target collection and construction of TCM regulatory network

The GeneCards database (<https://www.genecards.org/>) houses data on recognized target genes essential for CIPN therapy. The extracted genes were cross-referenced with the active ingredient's target genes to find common ground between the Xu Tongbi recipe and CIPN therapeutic goals. This was then visualized as a "disease-TCM-active ingredient-target" network, utilizing Cytoscape v3.7.0 software.

Construction of Protein Interaction Network

The screened targets were examined online using the Protein Interaction Network (PPI) on the String website (<https://string-db.org/cgi/input.pl>), where the confidence level annotated the interactions between the proteins. A score > 0.4 was considered significant. The proteins with the utmost correlation were screened based on each target gene's "node connection degree".

GO enrichment and KEGG pathway analysis of targets

GO enrichment and KEGG pathway analysis were conducted employing R software's "ClusterProfiler" package. The outcomes were ranked in descending order of P values and visualized as bubble charts for enhanced interpretability.

Mechanistic analysis

Quantitative Real-time PCR

Quantitative Real-time PCR was employed to assess the mRNA expression levels of the target genes. Briefly, two L4-6 DRG tissues were extracted from each rat and subjected to Trizole. The tissues were then homogenized at high speed. Post homogenization, the samples were centrifuged, the supernatant was mixed with isopropanol and centrifuged again, after which the supernatant was discarded. The residues were washed with 75% ethanol and centrifuged, the procedure being repeated once. The samples were mildly dried at 4°C before adding 30 µL of RNase-free water. The RNA concentrations were ascertained using a spectrophotometer. The acquired RNA was then reverse-transcribed into cDNA using a Real-Time PCR kit following the manufacturer's guidelines. Primers, at a concentration of 4 µM, were added to the corresponding PCR reaction mixture to achieve a total reaction volume of 25 µL, initiating the Real-

Time PCR reaction. The amplification and dissolution curves of Real-Time PCR were inspected, and the qPCR data were analyzed with SPSS software.

Western Blot to detect the protein expression level of the target gene

Two dorsal root ganglion tissues from levels L4-6 were harvested from each rat. These tissues were mixed with RIPA lysis buffer and subsequently disrupted using a high-speed mechanical homogenizer to obtain the supernatant. The concentration of proteins in the supernatant was quantified utilizing the BCA protein assay kit. This protein solution was subjected to electrophoretic separation on an SDS-PAGE gel. Following their separation, the proteins were subsequently transferred to polyvinylidene difluoride (PVDF) membranes (Millipore, USA). These membranes were blocked using the blocking buffer (5% skimmed milk). Following this, the PVDF membranes were incubated with anti-PDX1 primary antibodies (1:1000 Bcl-2, 1:1000 Bcl-2, 1:1000 PI3K, 1:1000 Akt, 1:10000 GAPDH) in a 3 ml solution at 4 °C with gentle shaking, overnight. After washing the membranes five times with TBS, they were incubated with the HRP-conjugated secondary antibody for 1 hour at room temperature. The intensities of the protein bands were quantified using ImageJ, supported by a professional image analysis system.

Results

General observations and animal behavior studies

Throughout animal testing, no abnormalities were observed in the skin on the feet or any other parts of rats exposed to the Hexu Tongbi formula. Any abnormal activity in the rats was attributed to peripheral neuropathy induced by oxaliplatin. Observations for erythema, rash, edema, breakage, and skin color appeared normal. The body weights of the different groups of rats were recorded and are represented in Figure 1A. On the 49th day, multiple comparison analysis (detailed in Table 3) revealed no significance in body weight between the normal control group, the model control group, and the Xu Tongbi recipe bath group ($P > 0.05$). Blood analyses were within normal ranges, showing normal liver, kidney, and myocardial functions, and no damage to the liver, kidneys, or heart was observed in any of the subjects.



Table-3. Multiple comparisons of the body weight of rats on the 49th day (the end of the experiment)

Group	Mean Diff.	95.00% CI of diff.		Adjusted P Value
Control vs. Model	98.27	41.8131	154.7297	0.002
Control vs. HXTB	99.37	42.9131	155.8297	0.002
Model vs. HXTB	1.100	-55.3583	57.5583	0.968

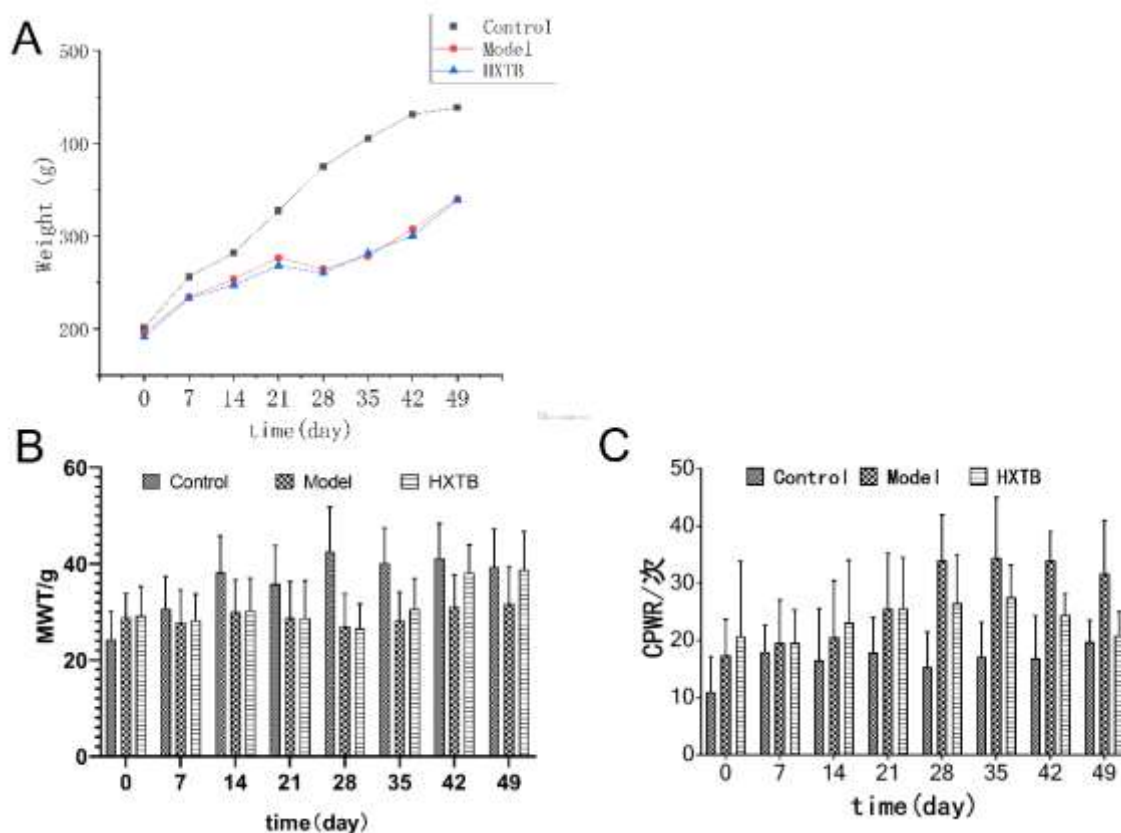


Figure-1: Weekly changes in rat body weight; each point represents the mean of 10 rat body weights in each group. (A). The effect of the Hexuetongbi formula on the threshold of mechanically stimulated foot withdrawal reflex, each bar represents the mean value of 10 MWT measurements of 10 rats in each group (B). The effect of the Hexuetongbi formula on the number of cold-stimulated withdrawal reflexes, each bar represents the average of cold-stimulated withdrawal times of 10 rats in each group (C).

The Mechanical Withdrawal Threshold (MWT) and the Cold-stimulated Paw Withdrawal Reflex (CPWR) were mainly observed in behavioral experiments. In the test examining the threshold of mechanical stimulation-induced foot withdrawal reflex, both the model control group and the Xuotongbi recipe bath group show distinct alterations during the model development period (0-28 days), as evidenced by the histogram and the results of multiple comparisons (Figure 1B), relative to the normal control group. Specifically, during the time of oxaliplatin treatment, the cumulative MWT, reflecting touch and hyperalgesia phenomena, was significantly reduced

in both mentioned groups. By the end of the modeling, on the 28th day (Table 4), the MWT of the normal control group was significantly higher compared to the other two groups ($P < 0.05$).

Starting from the 35th day, or the first week after the administration began, the MWT of the Xuotongbi recipe bath group began to increase incrementally. By the 49th day, the conclusion of the experiment (Table 5), its MWT did not show a significant difference compared to the normal control group ($P = 0.659 > 0.05$). A notable difference remained when compared with the model control group ($P < 0.05$).

After the discontinuation of oxaliplatin



administration, the model control group exhibited a slow recovery, with its MWT remaining significantly different from the other two groups after the trial concluded ($P < 0.05$).

Table-4: Multiple comparisons of the thresholds of mechanically stimulated paw withdrawal reflex in rats on day 28 (end of modeling)

Group	Mean Diff.	95.00% CI of diff.		Adjusted P Value
Control vs. Model	15.4839	13.07214	17.89563	0.000
Control vs. HXTB	15.9974	13.58562	18.40912	0.000
Model vs. HXTB	0.5135	-1.89826	2.92523	0.675

Table-5: Multiple comparisons of the withdrawal reflex threshold of mechanical stimulation on the 49th day (the end of the experiment) in rats

Group	Mean Diff.	95.00% CI of diff.		Adjusted P Value
Control vs. Model	7.6225	5.02288	10.22212	0.000
Control vs. HXTB	0.5835	-2.01612	3.18312	0.659
Model vs. HXTB	-7.0390	-9.63862	-4.43938	0.000

According to the histogram and the results of multiple comparisons (Figure 1C), the cold-stimulated-induced withdrawal reflex was compared in the normal control group, the model control group, and the Xuotongbi recipe bath group gradually increased during the modeling period (0-28 days). At the end of the oxaliplatin treatment on the 28th day, there was an increase in CPWR that was significantly different from the normal control group (Table 6) ($P < 0.05$). However, beginning on the 35th day after administration, the CPWR of the Xuotongbi recipe bath group gradually decreased. By the end of the experiment on the 49th day (Table 7), the Xuotongbi recipe bath group exhibited similar results as the normal control group ($P = 0.737 > 0.05$), which was significantly different from the model control group ($P = 0.0050 < 0.05$). However, the model control group recovered slowly following the discontinuation of oxaliplatin administration. The model control group's MWT significantly differed from the other two groups after the trial ($P < 0.05$).

Table-6: Multiple comparisons of cold-stimulated-induced withdrawal reflexes on day 28 (end of modeling) in rats

Group	Mean Diff.	95.00% CI of diff.		Adjusted P Value
Control vs. Model	-18.5714	-27.03091	-10.11195	0.000
Control vs. HXTB	-11.1429	-19.60234	-2.68338	0.013
Model vs. HXTB	7.4286	-1.03091	15.88805	0.082

Table-7: Multiple comparisons of cold-stimulated-induced withdrawal reflexes on day 49 (end of experiment) in rats

Group	Mean Diff.	95.00% CI of diff.		Adjusted P Value
Control vs. Model	-12.0000	-19.05150	-4.94850	0.002
Control vs. HXTB	-1.1429	-8.19436	5.90864	0.737
Model vs. HXTB	10.8571	3.80564	17.90864	0.005

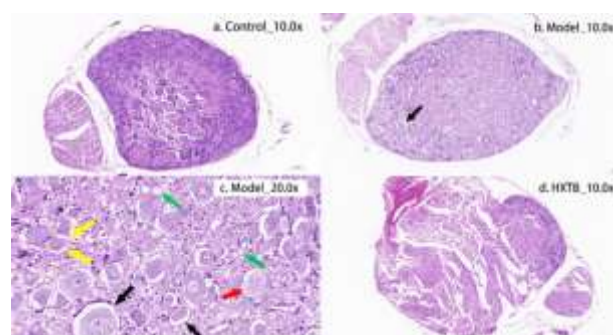


Figure-2. Microscopic examination of the L4-6 dorsal root ganglion tissue and cells in three groups: a. Control_10.0x: Control group under 10x microscope, b. Model_10.0x: Model group under 10x microscope, c. Model_20.0x: model group under 20x microscope, d. HXTB_10.0x: Hexuetong bath group under 10x microscope.

The effect of Hexuetongbi formula on rat L4-6 dorsal root ganglion tissue and cells

Neurons in the control and medicinal bath groups were plentiful and regularly distributed, as shown in Figures 2a and 2d, with obvious nucleocytoplasmic demarcation, nucleoli, and no visible inflammation. In the model group, neuronal cell bodies were more swollen (Fig. 2b). Under a 20x microscope (Fig. 2c), the gap between the cells grew (black arrows), and some neuron cell bodies and nuclei disappeared as a result of cytoplasmic lysis represented by red arrows.

Also, satellite cells were reduced around neuronal cell bodies (yellow arrows), and an increase in nerve fiber demyelination was observed.

Screening results of active ingredients and target genes of Hexuetongbi formula

The TCMSP database yielded 665 chemical constituents, including 12 types of AR, 192 types of ARER, 18 types of CAC, 220 types of CR, and 223 types of ADBEH. There are 3 types of active ingredients AR, 8 types of ARER, 3 types of CAC, 7 types of CR, 10 types of ADBEH, and 3 types of common ingredients, for a total of 27 active ingredients (see Appendix 1). According to the 27 active ingredients evaluated, 289 targets were acquired from the TCMSP database for each ingredient. After eliminating the common targets, 141 new targets remained.

Prediction of the effect of Hexuetongbi Recipe on CIPN

The Genecard database yielded a total of 375 target genes associated with CIPN. The acquired genes were compared with the screened target genes of

chemical constituents to determine the intersection (Fig. 3A). For the therapy of CIPN, Hexuetongbi Formula yielded a total of thirty-five targets. Again, 8 active ingredients that could not correspond to the common targets were eliminated by comparison. The obtained 35 common targets and 19 active ingredients of traditional Chinese medicine were imported into Cytoscape v3.7.0 software, and the "disease-traditional Chinese medicine-active ingredients-target" network diagram was constructed (Figure 3B). In the illustration, active ingredients are denoted by blue nodes, common illnesses and drug targets are represented by yellow nodes, and the gray lines signify the interactions between active ingredients and targets. As illustrated in the picture, each active ingredient correlates to many targets. Each target gene corresponds to several active ingredients, reflecting the complexity of Hexuetongbi Recipe's mechanism of action in treating CIPN. Then, using the String website, 35 protein targets were assessed by the PPI of target genes, a PPI network was formed (Figure 3C), and the top 20 protein targets with the highest correlation in the network were screened according to degree. (see Figure 3D).

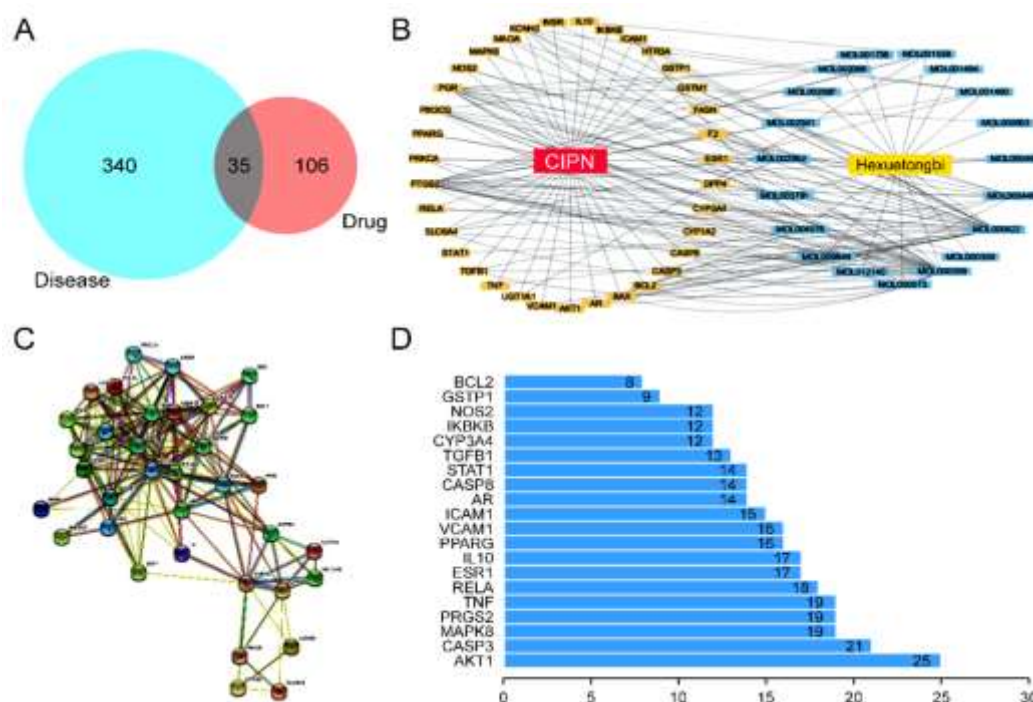


Figure-3. Matching of CIPN target and Hexuetongbi target (A). "Disease-Chinese medicine-active ingredient-target" network diagram (B). Protein interaction network diagram (C). Top 20 most relevant protein targets (D).

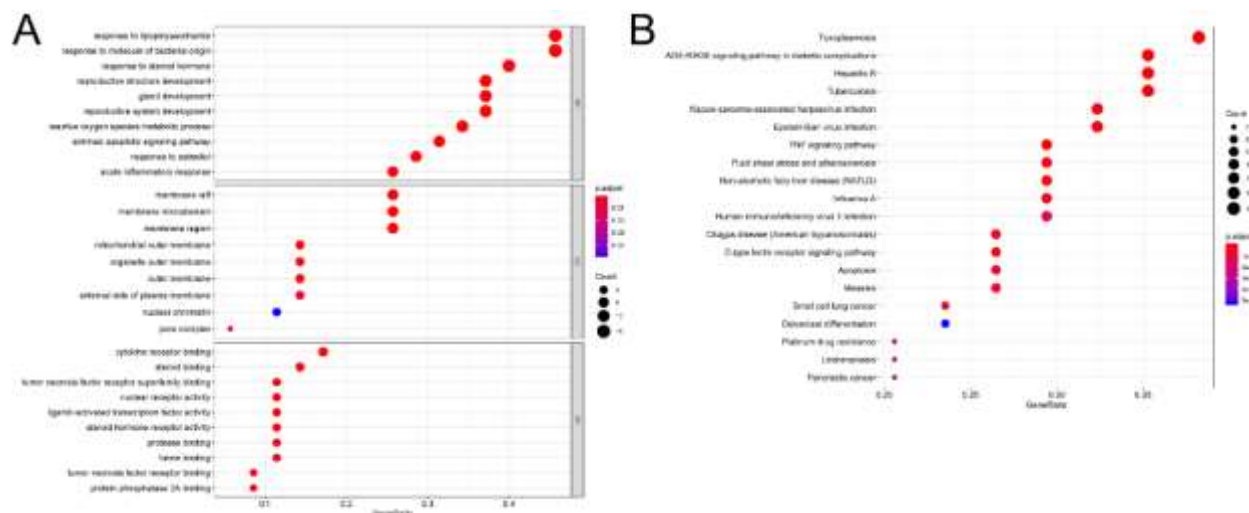


Figure-4. GO enrichment analysis (A). KEGG enrichment analysis (B)

GO enrichment analysis and KEGG pathway analysis of targets

The GO enrichment analysis is shown in Figure 4A. Numerous enriched genes were found in the biological process (BP) study, such as those that respond to lipopolysaccharides, molecules of bacterial origin, steroid hormones, etc. There are many enriched genes in the analysis of cellular components (CC), including membrane microdomain, membrane region, and membrane raft. Numerous enriched genes were identified using molecular function (MF) analysis, such as those involved in binding tumor necrosis factor receptor superfamily members, steroids, and cytokine receptors. Based on the findings of a KEGG pathway enrichment analysis, the pathways that demonstrate the highest levels of correlation and enrichment are primarily the AGE-RAGE signaling pathway in diabetic complications, the TNF signaling pathway, the C-type lectin receptor signaling pathway, and apoptosis (Figure 4B) after conducting additional research on the pathway maps of the pathways mentioned above and taking into account the most critical targets in the protein interaction network. Conclusively, the three pathways of PI3K-Akt, JNK/MAPK, and COX-2 (PTGS2) may be the most closely related to treating CIPN with Hexuetongbi Recipe.

The effect of Hexuetongbi on the mRNA expression levels of PI3K, Akt1, Akt2, Akt3, MAPK8, PTGS2, Bcl-2 and the effects on PI3K, Akt (phospho S473), Bcl-2 effect on protein expression levels.

As depicted in the figure and table (Figure 5A, Table 8), there were significant differences in the PI3K index between the three groups ($P < 0.05$), and the mRNA expression of Akt1 and Akt3 was significantly lower in the model control group than in the normal control group and Xuetingbi recipe bath group. There was no significant difference ($P > 0.05$) between the normal control and Xuetingbi bath groups. Akt3, MAPK8, and PTGS2 were upregulated, but no difference existed between the medicated bath group and the normal control group ($P > 0.05$). PI3K, Akt1, and Akt3 can inhibit cell apoptosis; their high expression levels can prevent cell apoptosis. The mRNA expression of the downstream target Bcl-2 determines whether nerve cells are affected by the inhibitory apoptosis pathway. The expression levels of Bcl-2 in the three groups were all significantly different ($P < 0.05$), as shown in the figures and tables (Fig. 5B, Table 8). The Western blot detection results are shown (Figure 5C, Table 9). The protein expression levels of PI3K, Akt (phospho S473), and Bcl-2 were significantly different between the Xuetingbi recipe bath group and the model group ($P < 0.05$).



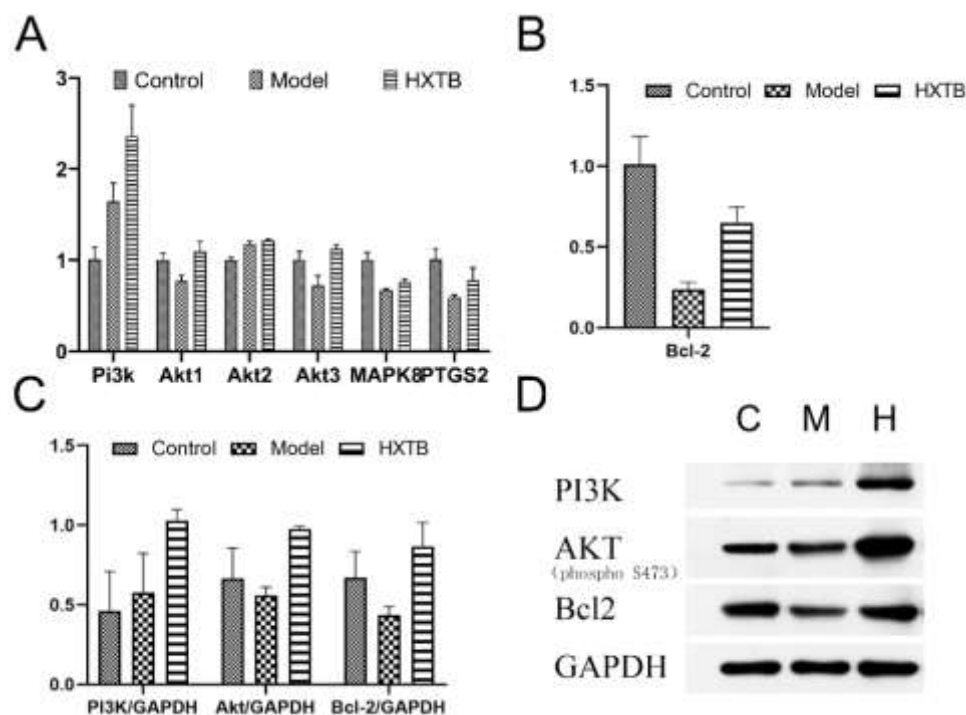


Figure-5. mRNA expression levels of PI3K, Akt1, Akt2, Akt3, MAPK8, and PTGS2 in rat L4-6 dorsal root ganglia (A). mRNA expression levels of Bcl-2 in rat L4-6 dorsal root ganglia (B). PI3K, Akt (phospho S473), and Bcl-2 expression levels in L4-6 dorsal root ganglia (C-D).

Table-8. Multiple comparison of mRNA expression of PI3K, Akt1, Akt2, Akt3, MAPK8, PTGS2, Bcl-2 in rat L4-6 dorsal root ganglion

Target	Group	Mean Diff.	95.00% CI of diff.	P
PI3K	Control vs. Model	-0.6389	-1.1152 to -0.1626	0.017
	Control vs. HXTB	-1.356	-1.8319 to -0.8793	0.000
	Model vs. HXTB	-0.7167	-1.1930 to -0.2404	0.010
Akt1	Control vs. Model	0.2314	0.0608 to 0.4020	0.016
	Control vs. HXTB	-0.0900	-0.2606 to 0.0806	0.244
	Model vs. HXTB	-0.3214	-0.4921 to -0.1509	0.004
Akt2	Control vs. Model	-0.1725	-0.2273 to -0.1177	0.000
	Control vs. HXTB	-0.2136	-0.2683 to -0.1588	0.000
	Model vs. HXTB	-0.0411	-0.0958 to 0.0137	0.116
Akt3	Control vs. Model	0.2821	0.1090 to 0.4552	0.007
	Control vs. HXTB	-0.1178	-0.2909 to 0.0553	0.147
	Model vs. HXTB	-0.3999	-0.5730 to -0.2268	0.001
MAPK8	Control vs. Model	0.3315	0.2279 to 0.4352	0.000
	Control vs. HXTB	0.2404	0.1368 to 0.3441	0.001
	Model vs. HXTB	-0.0910	-0.1948 to 0.0126	0.075
PTGS2	Control vs. Model	0.4138	0.2006 to 0.6272	0.003
	Control vs. HXTB	0.2277	0.0145 to 0.4411	0.040
	Model vs. HXTB	-0.1861	-0.3994 to 0.0272	0.077
Bcl-2	Control vs. Model	0.7725	0.5371 to 1.0079	0.000
	Control vs. HXTB	0.3620	0.1266 to 0.5974	0.009
	Model vs. HXTB	-0.4105	-0.6459 to -0.1751	0.005



Table-9. Multiple comparison of PI3K, Akt (phospho S473) and Bcl-2 protein expression in rat L4-6 dorsal root ganglia

Target	Group	Mean Diff.	95.00% CI of diff.	P
PI3K	Control vs. Model	-0.1163	-0.5299 to 0.2974	0.517
	Control vs. HXTB	-0.5696	-0.9833 to -0.1559	0.015
	Model vs. HXTB	-0.4533	-0.8670 to -0.0396	0.036
Akt1 (phospho S473)	Control vs. Model	0.1078	-0.1214 to 0.3371	0.293
	Control vs. HXTB	-0.3107	-0.5399 to -0.0815	0.016
	Model vs. HXTB	-0.4186	-0.6478 to -0.1893	0.004
Bcl-2	Control vs. Model	0.2364	-0.0279 to 0.5009	0.071
	Control vs. HXTB	-0.1948	-0.4592 to 0.0696	0.122
	Model vs. HXTB	-0.4312	-0.6957 to -0.1668	0.007

Discussion

In our study of the Hexuetongbi formula, we primarily explored its potential therapeutic effects for CIPN. In current CIPN management, duloxetine is a widely accepted standard treatment. It is one of the few pharmacologic agents specifically recommended for CIPN due to its effectiveness in mitigating pain symptoms. This recommendation is backed by the ASCO guidelines, which highlight duloxetine for its clinically significant reduction in pain, although it is associated with side effects such as fatigue and dizziness (Hershman et al., 2014; Loprinzi et al., 2020).

Additionally, emerging therapies like mirogabalin have been assessed in clinical trials, showing promise in managing CIPN symptoms effectively. For instance, the MiroCIP study illustrates mirogabalin's potential, demonstrating its safety and efficacy in reducing neuropathic pain, which could make it a valuable part of the CIPN treatment arsenal (Misawa et al., 2023).

Our research suggests that Hexuetongbi might offer a multifaceted approach by not only targeting symptomatic relief but also potentially modulating underlying biological pathways involved in neuropathy, such as the PI3K/Akt signaling pathway, which is noted for its role in cell survival and apoptosis. While these findings are preliminary, they underscore the need for further research to validate the efficacy and safety of Hexuetongbi compared to these established therapies.

By drawing on TCM, Hexuetongbi could provide a novel integrative treatment option that complements existing pharmacological therapies, potentially offering fewer side effects and improved patient tolerance. CIPN is a common side effect of platinum-containing chemotherapeutics such as oxaliplatin.

Oxaliplatin can cause neuronal cell damage by directly affecting a number of genes and pathways, such as the BCL-2 family on the apoptosis pathway, and activating the expression of p38, ERK1/2, and JNK/SapK in the MAPK signaling pathway, resulting in neuronal apoptosis (Scuteri et al., 2009). The dorsal root ganglion is the predominant site of action for platinum-induced neurotoxicity (Jongen et al., 2015). Platinum drugs can inhibit rRNA synthesis in neurons' nuclei, thus reducing the ability of protein synthesis, resulting in abnormal organelles and morphological changes in neurons.

In this study, we revealed that using Hexuetongbi Formula, tactile sensation and hyperalgesia were gradually improved in the rat model of oxaliplatin-induced peripheral neuropathy. The pathological sections of the rat dorsal root ganglion were examined, and it was observed that the dorsal root ganglion cells of the oxaliplatin rat model, without the intervention of the Hexuetongbi recipe, were significantly damaged. In contrast, the dorsal root ganglion cells of the oxaliplatin rat model were damaged without the intervention of the Hexuetongbi recipe. The morphology of neurons in the dorsal root ganglia of rats treated with the Xuetongbi recipe tended to be normal, with no obvious cell damage. Following that, we found the active ingredients of Hexuetongbi Formula using TCMSP. According to the literature, in a tail dipping experiment, neocytine in Chuanwu has an antinociceptive effect on the reticular nucleus of giant cells in rats. Benzoylneocytine in aconitum has been shown to have a dose-dependent antinociceptive effect on neurons (Hikino and Murayama, 1985; Suzuki et al., 1994), and diterpene alkaloids have analgesic properties by modulating opioid receptors (Nesterova et al., 2014). Asarum contains methyl eugenol, an effective anesthetic, anticonvulsant, and analgesic



component (Sayyah et al., 2002; Sell and Carlini, 1976; Yano et al., 2006). Lignans derived from Chuanmutong exhibit anti-neuritic properties, effectively suppressing the secretion of inflammatory mediators, NO and TNF, in the inflammatory cascade of BV-2 cells stimulated by lipopolysaccharide (Xiong et al., 2014).

The administration of an extract derived from cinnamon twigs has been found to mitigate neuroinflammation. This effect is achieved by downregulating the TLR4/MyD88 signaling pathway. Concurrently, there is a reduction in the secretion of inflammatory mediators such as NO, IL-6, IL-1, and TNF (Hwang et al., 2009; Yang et al., 2017). Angelica dahurica's furanocoumarin can regulate the TRPV1 channel, significantly inhibit the plantar neurotoxicity of rats caused by formalin, and inhibit pain (Chen et al., 2014). Additionally, it can eradicate ROS by activating the PI3K/Akt/NF- pathway. Reduce the damage caused by oxidative stress and exert cytoprotective effects (Kang et al., 2019; Lee et al., 2011; Wang et al., 2017). These five traditional Chinese medicines reduce nerve cell damage, offer additional analgesia, and have anti-inflammatory properties. Following identifying these components that can protect nerve cells, we identified three pathways, PI3K-Akt, JNK/MAPK, and COX-2 (PTGS2), most likely to affect nerve cells by Hexuetongbi recipe. The mRNA expression levels of PI3K/Akt, MAPK8, and PTGS2 were determined through molecular mechanism studies. Herein, the mRNA expression levels of PI3K, Akt1, and Akt3 were significantly upregulated, while MAPK8 and PTGS2 were unaffected. The protein expression levels of PI3K and Akt (phospho S473) were then determined to be statistically significant, and their up-regulation was significant, consistent with the mRNA expression trend.

The PI3K/Akt pathway regulates cell survival, apoptosis, and differentiation and is vital in biological processes by regulating the Bcl-2 apoptosis-related family proteins. Several studies have demonstrated that activating the PI3K/Akt pathway can protect nerve cells (Abbruzzese et al., 2020; Limbourg et al., 2003; Sisalli et al., 2014; Zhao et al., 2016) and reduce oxidative damage to nerve cells (Hao and Rockwell, 2013; Zhou et al., 2008). The findings suggest that the Hexuetongbi recipe can inhibit apoptosis of neuronal cells in the dorsal root ganglia via the PI3K/Akt pathway, thus further improving oxaliplatin-induced peripheral neuropathy,

even in the presence of neuronal cell damage and promoting nerve repair.

TCM is of natural origin and is increasingly recognized worldwide for treating CIPN. The research on the treatment mechanism of TCM compounds will aid in creating new therapeutic approaches for CIPNs. These new therapeutic approaches will help improve the occurrence and development of CIPN and reduce the pain that patients experience. According to the findings of this study, the Hexuetongbi recipe can significantly improve oxaliplatin-induced peripheral neuropathy in rats, reduce the phenomenon of touch and hyperalgesia, and improve as well as reduce the damage caused by oxaliplatin to peripheral neurons. Our findings provide a substantial foundation for future research into alternative treatments. This study highlights the potential of TCM to offer efficacious alternatives or adjuncts to conventional pharmacological approaches, particularly for patients experiencing side effects or inadequate relief from current CIPN treatments. The network pharmacology approach used here underscores the value of exploring complex biological interactions and could lead to the identification of novel therapeutic targets. Firstly, clinical trials should be conducted to validate the efficacy and safety of the formula in a broader, clinically diverse population. These trials could focus on dosing strategies, long-term effects, and comparative studies against current standard treatments. Additionally, further investigations into the molecular mechanisms of action of Hexue Tongbi could provide deeper insights into its therapeutic targets and potential synergies with other therapies. Understanding the bioactive compounds within the formula and their interactions with cellular pathways relevant to neuropathy could lead to the development of more targeted therapies for CIPN.

While our study presents promising preliminary results on the efficacy of the Hexuetongbi formula in managing symptoms of CIPN through mechanisms such as the modulation of the PI3K/Akt signaling pathway, it is essential to recognize the inherent limitations and potential biases that could affect the interpretation of these findings. Using a relatively small sample size may not fully capture the variability in treatment response across a diverse patient population, and the study design, which may lack randomization or control groups, could introduce biases. Additionally, our focus on symptom relief as the primary outcome may not



provide a comprehensive view of the full spectrum of neuropathy effects. The inclusion of more extensive neurophysiological assessments and quality-of-life measures could enrich our understanding of the treatment's impact. Furthermore, the follow-up period in this study might not be sufficient to observe the long-term effects and potential side effects of the Hexuetongbi treatment, suggesting that future studies should include longer follow-up durations. Considering these factors, larger-scale, randomized controlled trials with longer follow-up and a broader range of outcome measures are recommended to validate our findings and minimize potential confounding factors, thereby providing a more robust basis for evaluating the therapeutic potential of the Hexuetongbi formula in CIPN management.

Conclusion

Our study elucidates the critical role of the PI3K/Akt signaling pathway and its downstream Bcl-2 protein in mediating neuronal apoptosis, shedding light on the molecular mechanisms underlying peripheral nerve damage caused by oxaliplatin. The significant upregulation of Bcl-2 apoptosis family proteins in response to pathway modulation highlights their potential as therapeutic targets to alleviate oxaliplatin-induced neurotoxicity. Moreover, this study paves the way for novel therapeutic strategies, potentially enhancing the quality of life for patients undergoing oxaliplatin-based chemotherapy. Future research should focus on detailed pathway analysis and the development of specific inhibitors that can effectively target these mechanisms. Additionally, clinical trials are necessary to evaluate the safety and efficacy of these targeted therapies in human subjects. By furthering our understanding of the PI3K/Akt and Bcl-2 pathways, we aim to develop more precise interventions to prevent or mitigate the debilitating effects of CPIN.

Ethics Approval Statement

All animal trials followed the guidelines suggested by the Animal Ethics Committee and the experimental unit of Guangzhou University of Traditional Chinese Medicine under protocol No. SYXK-2017-0125.

Disclaimer: None.

Conflict of Interest: None.

Source of Funding: This work was financially supported by the 2020 Bao'an District Medical and

Health Basic Research Project (No. 2020JD498), the New Coronary Pneumonia Treatment and Epidemic Prevention and Control Technology Research and Application of Traditional Chinese Medicine (No. 2020KJCX-KTYJ-85).

Contribution of Authors

Feng J: Conceptualized the research, conducted the experiments, drafted the manuscript, reviewed and edited the manuscript

Yang L: Conducted the experiments, reviewed and edited the manuscript

Wang J & Zhang J: Carried out the data analysis

Lin L: Conceptualized the research, reviewed and edited the manuscript, supervised the entire research and provided funding for the project.

References

- Abbruzzese G, Morón-Oset J, Díaz-Castroverde S, García-Font N, Roncero C, López-Muñoz F, Marco Contelles JL and Oset-Gasque MJ, 2020. Neuroprotection by phytoestrogens in the model of deprivation and resupply of oxygen and glucose in vitro: the contribution of autophagy and related signaling mechanisms. *Antioxidants*. 9: 545
- Albers JW, Chaudhry V, Cavaletti G and Donehower RC, 2014. Interventions for preventing neuropathy caused by cisplatin and related compounds. *Cochrane Database Syst. Rev*. 3.
- Argyriou AA, 2015. Updates on oxaliplatin-induced peripheral neurotoxicity (OXAIPN). *Toxics*. 3: 187–197.
- Argyriou AA, Bruna J, Marmioli P and Cavaletti G, 2012. Chemotherapy-induced peripheral neurotoxicity (CIPN): an update. *Crit. Rev. Oncol. Hematol*. 82: 51–77.
- Argyriou AA, Polychronopoulos P, Iconomou G, Chroni E and Kalofonos HP, 2008. A review on oxaliplatin-induced peripheral nerve damage. *Cancer Treat. Rev*. 34 368–77
- Chen X, Sun W, Gianaris NG, Riley AM, Cummins TR, Fehrenbacher JC and Obukhov AG, 2014. Furanocoumarins are a novel class of modulators for the transient receptor potential vanilloid type 1 (TRPV1) channel. *J. Biol. Chem*. 289: 9600–9610.
- Chien TJ, Liu CY, Fang CJ and Kuo CY, 2019. The



- Efficacy of Acupuncture in Chemotherapy-Induced Peripheral Neuropathy: Systematic Review and Meta-Analysis. *Integr. Cancer Ther.* 18: 1534735419886662.
- Delaunoy T, Alberts SR, Sargent DJ, Green E, Goldberg RM, Krook J, Fuchs C, Ramanathan RK, Williamson SK and Morton RF, 2005. Chemotherapy permits resection of metastatic colorectal cancer: experience from Intergroup N9741. *Ann. Oncol.* 16: 425–429.
- Gamelin L, Boisdron-Celle M, Morel A, Poirier AL, Berger V, Gamelin E, Tournigand C and de Gramont A, 2008. Oxaliplatin-related neurotoxicity: interest of calcium-magnesium infusion and no impact on its efficacy. *J. Clin. Oncol.* 26: 1188–1189.
- Hao T and Rockwell P, 2013. Signaling through the vascular endothelial growth factor receptor VEGFR-2 protects hippocampal neurons from mitochondrial dysfunction and oxidative stress. *Free Radic. Biol. Med.* 63: 421–431.
- Heinemann V, Haas M and Boeck S, 2012. Systemic treatment of advanced pancreatic cancer. *Cancer Treat. Rev.* 38: 843–853.
- Hershman DL, Lacchetti C, Dworkin RH, Lavoie Smith EM, Bleeker J, Cavaletti G, Chauhan C, Gavin P, Lavino A and Lustberg MB, 2014. Prevention and management of chemotherapy-induced peripheral neuropathy in survivors of adult cancers: American Society of Clinical Oncology clinical practice guideline. *J. Clin. Oncol.* 32: 1941–1967.
- Hikino H and Murayama M, 1985. Mechanism of the antinociceptive action of mesaconitine: participation of brain stem and lumbar enlargement. *Br. J. Pharmacol.* 85: 575–580.
- Holmes J, Stanko J, Varchenko M, Ding H, Madden VJ, Bagnell CR, Wyrick SD and Chaney SG, 1998. Comparative neurotoxicity of oxaliplatin, cisplatin, and ormaplatin in a Wistar rat model. *Toxicol. Sci.* 46: 342–351.
- Hochster HS, 2007. Use of calcium and magnesium salts to reduce oxaliplatin-related neurotoxicity. *J. Clin. Oncol.* 25: 4028–4029.
- Hwang SH, Choi YG, Jeong MY, Hong YM, Lee JH and Lim S, 2009. Microarray analysis of gene expression profile by treatment of Cinnamomi Ramulus in lipopolysaccharide-stimulated BV-2 cells. *Gene.* 443: 83–90.
- Jasmin L, Kohan L, Franssen M, Janni G and Goff JR, 1998. The cold plate as a test of nociceptive behaviors: description and application to the study of chronic neuropathic and inflammatory pain models. *Pain.* 75: 367–382.
- Jongen JLM, Broijl A and Sonneveld P, 2015. Chemotherapy-induced peripheral neuropathies in hematological malignancies. *J. Neurooncol.* 121: 229–237.
- Kang U, Han AR, So Y, Jin CH, Ryu SM, Lee D and Seo EK, 2019. Furanocoumarins from the Roots of *Angelica dahurica* with Inhibitory Activity against Intracellular Reactive Oxygen Species Accumulation. *J. Nat. Prod.* 82: 2601–2607.
- Lee MY, Lee JA, Seo CS, Ha H, Lee H, Son JK and Shin HK, 2011. Anti-inflammatory activity of *Angelica dahurica* ethanolic extract on RAW264.7 cells via upregulation of heme oxygenase-1. *Food Chem. Toxicol.* 49: 1047–1055.
- Limbourg FP, Huang Z, Plumier JC, Simoncini T, Fujioka M, Tuckermann J, Schütz G, Moskowitz MA and Liao JK, 2003. Rapid nontranscriptional activation of endothelial nitric oxide synthase mediates increased cerebral blood flow and stroke protection by corticosteroids. *J. Clin. Invest.* 111: 759.
- Liu H, Wang J, Zhou W, Wang Y and Yang L, 2013. Systems approaches and polypharmacology for drug discovery from herbal medicines: an example using licorice. *J. Ethnopharmacol.* 146: 773–793.
- Liu X, Ou K, Ma X, Gao L, Wang Q, Zhang H and Yang L, 2022. Safety and efficacy of irinotecan, oxaliplatin, and capecitabine (XELOXIRI) regimen with or without targeted drugs in patients with metastatic colorectal cancer: a retrospective cohort study. *BMC Cancer.* 22: 807.
- Loprinzi CL, Lacchetti C, Bleeker J, Cavaletti G, Chauhan C, Hertz DL, Kelley MR, Lavino A, Lustberg MB, Paice JA, Schneider BP, Lavoie Smith EM, Smith ML, Smith TJ, Wagner-Johnston N and Hershman DL, 2020. Prevention and Management of Chemotherapy-Induced Peripheral Neuropathy in Survivors of Adult Cancers: ASCO Guideline Update. *J. Clin. Oncol.* 38: 3325–3348.
- Loprinzi CL, Qin R, Dakhil SR, Fehrenbacher L, Flynn KA, Atherton P, Seisler D, Qamar R, Lewis GC and Grothey A, 2014. Phase III randomized, placebo-controlled, double-blind study of intravenous calcium and magnesium to



- prevent oxaliplatin-induced sensory neurotoxicity (N08CB/Alliance). *J. Clin. Oncol.* 32: 997.
- Lu W, Giobbie-Hurder A, Freedman RA, Shin IH, Lin NU, Partridge AH, Rosenthal DS and Ligibel JA, 2020. Acupuncture for Chemotherapy-Induced Peripheral Neuropathy in Breast Cancer Survivors: A Randomized Controlled Pilot Trial. *The Oncologist.* 25: 310–318.
- Mannelli LDC, Zanardelli M, Failli P and Ghelardini C, 2012. Oxaliplatin-induced neuropathy: oxidative stress as pathological mechanism. Protective effect of silibinin. *J. Pain.* 13: 276–284.
- Misawa S, Denda T, Kodama S, Suzuki T, Naito Y, Kogawa T, Takada M, Suichi T, Shiosakai K, Kuwabara S, Saito G, Hino A, Imanishi S, Ureshino N, Satomi D, Tanabe Y, Hanaoka Y, Miyamoto A, Suzuki T, Naganuma A, Yanagita Y, Sekine K, Kusano F, Nakamura M, Imazeki H and on behalf of the MiroCIP study group, 2023. Efficacy and safety of mirogabalin for chemotherapy-induced peripheral neuropathy: a prospective single-arm trial (MiroCIP study). *BMC Cancer.* 23: 1098.
- Nara K, Yamamoto T, Yamashita H, Yagi K, Takada T, Seto Y and Suzuki H, 2023. Prior treatment with oxaliplatin-containing regimens and higher total bilirubin levels are risk factors for neutropenia and febrile neutropenia in patients with gastric or esophagogastric junction cancer receiving weekly paclitaxel and ramucirumab therapy: a single center retrospective study. *BMC Cancer.* 23: 979.
- National Research Council (US) Committee for the Update of the Guide for the care and Use of Laboratory Animals, 2011. *Guide for the Care and Use of Laboratory Animals* (Washington (DC): National Academies Press (US)). Online: <http://www.ncbi.nlm.nih.gov/books/NBK54050/>
- Nesterova YV, Povet'yeva TN, Suslov NI, Zyuz'kov GN, Pushkarskii SV, Aksinenko SG, Schultz EE, Kravtsova SS and Krapivin AV, 2014. Analgesic activity of diterpene alkaloids from *Aconitum baikalensis*. *Bull. Exp. Biol. Med.* 157: 488.
- Sasako M, Sakuramoto S, Katai H, Kinoshita T, Furukawa H, Yamaguchi T, Nashimoto A, Fujii M, Nakajima T and Ohashi Y, 2011. Five-Year Outcomes of a Randomized Phase III Trial Comparing Adjuvant Chemotherapy With S-1 Versus Surgery Alone in Stage II or III Gastric Cancer. *J. Clin. Oncol.* 29: 4387–4393.
- Sayyah M, Valizadeh J and Kamalinejad M, 2002. Anticonvulsant activity of the leaf essential oil of *Laurus nobilis* against pentylenetetrazole-and maximal electroshock-induced seizures. *Phytomedicine.* 9: 212–216.
- Scuteri A, Galimberti A, Maggioni D, Ravasi M, Pasini S, Nicolini G, Bossi M, Miloso M, Cavaletti G and Tredici G, 2009. Role of MAPKs in platinum-induced neuronal apoptosis. *Neurotoxicology.* 30: 312–319.
- Sell AB and Carlini EA, 1976. Anesthetic action of methyleugenol and other eugenol derivatives. *Pharmacology.* 14: 367–377.
- Sisalli MJ, Secondo A, Esposito A, Valsecchi V, Savoia C, Di Renzo GF, Annunziato L and Scorziello A, 2014. Endoplasmic reticulum refilling and mitochondrial calcium extrusion promoted in neurons by NCX1 and NCX3 in ischemic preconditioning are determinant for neuroprotection. *Cell Death Differ.* 21: 1142–1149.
- Smith EML, Pang H, Cirrincione C, Fleishman S, Paskett ED, Ahles T, Bressler LR, Fadul CE, Knox C, Le-Lindqwister N, Gilman PB and Shapiro CL, 2013. Effect of duloxetine on pain, function, and quality of life among patients with chemotherapy-induced painful peripheral neuropathy: a randomized clinical trial. *JAMA* 309: 1359–1367.
- Staff NP, Grisold A, Grisold W and Windebank A J, 2017. Chemotherapy-induced peripheral neuropathy: a current review. *Ann. Neurol.* 81: 772–781.
- Suzuki Y, Oyama T, Ishige A, Isono T, Asami A, Ikeda Y, Noguchi M and Omiya Y, 1994. Antinociceptive mechanism of the Actonitine alkaloids mesaconitine and benzoylmesaconine. *Planta Med.* 60: 391–394.
- Wang KS, Lv Y, Wang Z, Ma J, Mi C, Li X, Xu GH, Piao LX, Zheng SZ and Jin X, 2017. Imperatorin efficiently blocks TNF- α -mediated activation of ROS/PI3K/Akt/NF- κ B pathway. *Oncol. Rep.* 37: 3397–3404.
- Xiong J, Bui VB, Liu XH, Hong ZL, Yang GX and Hu JF, 2014. Lignans from the stems of *Clematis armandii* (“Chuan-Mu-Tong”) and their anti-neuroinflammatory activities. *J. Ethnopharmacol.* 153: 737–743.
- Yang H, Cheng X, Yang Y, Wang Y and Du G, 2017. *Ramulus Cinnamomi* extract attenuates neuroinflammatory responses via downregulating

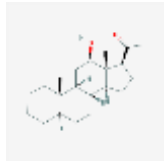
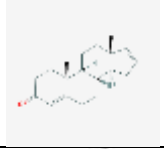
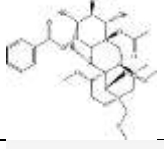
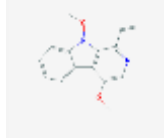
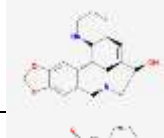
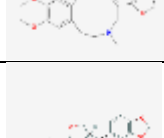

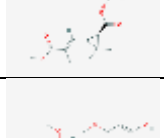




- TLR4/MyD88 signaling pathway in BV2 cells. *Neural Regen. Res.* 12: 1860.
- Yano S, Suzuki Y, Yuzurihara M, Kase Y, Takeda S, Watanabe S, Aburada M and Miyamoto K, 2006. Antinociceptive effect of methyleugenol on formalin-induced hyperalgesia in mice. *Eur. J. Pharmacol.* 553: 99–103.
- Zhao H, Mitchell S, Koumpa S, Cui YT, Lian Q, Hagberg H, Johnson MR, Takata M and Ma D, 2016. Heme oxygenase-1 mediates neuroprotection conferred by argon in combination with hypothermia in neonatal hypoxia–ischemia brain injury. *Anesthesiology*. 125: 180–192.
- Zheng FY, Xiao WH and Bennett GJ, 2011. The response of spinal microglia to chemotherapy-evoked painful peripheral neuropathies is distinct from that evoked by traumatic nerve injuries. *Neuroscience*. 176: 447–454.
- Zhou J, Zhang S, Zhao X and Wei T, 2008. Melatonin impairs NADPH oxidase assembly and decreases superoxide anion production in microglia exposed to amyloid- β 1–42. *J. Pineal Res.* 45: 157–165.



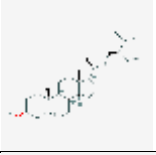
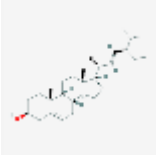
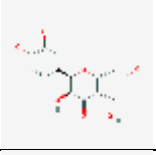

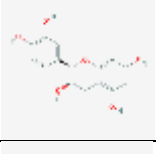

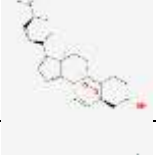





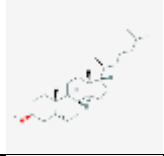
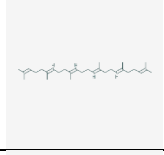
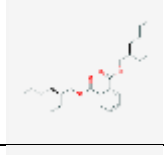
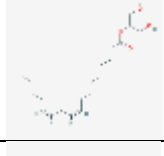

Appendix 1

Active Ingredients of Hexuetongbi Formula

ID	Name	Molecular formula	OB(%)	DL	Drug
MOL002086	1-[(5R,8R,9S,10S,12R,13S,14S,17S)-12-hydroxy-10,13-dimethyl-2,3,4,5,6,7,8,9,11,12,14,15,16,17-tetradecahydro-1H-cyclopenta[a]phenanthren-17-yl] ethanone		33.47	0.42	AR
MOL002087	delta4,16-Androstadien-3-one		37.63	0.31	AR
MOL000538	hypaconitine		31.39	0.26	AR
MOL012140	4,9-dimethoxy-1-vinyl-\$b\$-carboline		65.3	0.19	ARER
MOL012141	Caribine		37.06	0.83	ARER
MOL001460	Cryptopin		78.74	0.72	ARER
MOL001558	sesamin		56.55	0.83	ARER
MOL002501	[(1S)-3-[(E)-but-2-enyl]-2-methyl-4-oxo-1-cyclopent-2-enyl] (1R,3R)-3-[(E)-3-methoxy-2-methyl-3-oxoprop-1-enyl]-2,2-dimethylcyclopropane-1-carboxylate		62.52	0.31	ARER
MOL002962	(3S)-7-hydroxy-3-(2,3,4-trimethoxyphenyl)chroman-4-one		48.23	0.33	ARER
MOL000422	kaempferol		41.88	0.24	ARER



MOL009849	ZINC05223929		31.57	0.83	ARER
MOL000358	beta-sitosterol		36.91	0.75	CAC
MOL000359	sitosterol		36.91	0.75	CAC
MOL000449	Stigmasterol		43.83	0.76	CAC
MOL001736	(-)-taxifolin		60.51	0.27	CR
MOL000492	(+)-catechin		54.83	0.24	CR
MOL000073	ent-Epicatechin		48.96	0.24	CR
MOL004576	taxifolin		57.84	0.27	CR
MOL011169	Peroxyergosterol		44.39	0.82	CR
MOL001494	Mandenol		42	0.19	ADBEH
MOL002883	Ethyl oleate (NF)		32.4	0.19	ADBEH

MOL005802	propyleneglycol monooleate		37.6	0.26	ADBEH
MOL000953	CLR		37.87	0.68	ADBEH
MOL001506	Supraene		33.55	0.42	ADBEH
MOL001749	ZINC03860434		43.59	0.35	ADBEH
MOL003791	Linolein, 2-mono-		37.28	0.3	ADBEH
MOL007514	methyl icoso-11,14-dienoate		39.67	0.23	ADBEH